Enhanced electrical characteristics of Zr/diamond Schottky barrier diode with cerium hexaboride interfacial layer

Tian-Fei Zhu [a,*], Guoqing Shao [a], Tai Min [b], Hong-Xing Wang [a]

[a] Key Lab for Physical Electronics and Devices of the Ministry of Education, Faculty of Electronics and Information Engineering, Xi'an Jiaotong University, Xi'an 710049, China
[b] Spintronic Materials and Quantum Devices Research Center, Xi'an Jiaotong University, Xi'an 710049, China

A B S T R A C T

To fabricate a performance-enhanced Schottky barrier diode (SBD) on a diamond, a cerium hexaboride (CeB_6) interfacial layer was introduced between the diamond and the Zr/Au electrode. The inserted CeB_6 layer was characterized using X-ray photoelectron spectroscopy. Introducing the CeB_6 layer significantly improved the performance of the diamond SBD compared with a sample without the layer. The ideality factor (n)/SBH (Φ_B) values of the SBD with and without the CeB_6 interlayer were 2.24/1.92 eV and 2.82/1.65 eV, representing an improvement of 20.5% and 16.4% for the ideality factor and Schottky barrier height, respectively. The reverse breakdown voltage increased from −86 to −110.5 V, indicating an improvement of 28.5% for breakdown voltage. Additionally, the reverse current of the SBD with CeB_6 was suppressed, making it more reliable and stable than that without CeB_6 before the breakdown threshold. The carrier concentration and depletion layer width were increased from 1.135×10^{14} cm^{-3} and 206.7 nm to 2.646×10^{14} cm^{-3} and 227.6 nm, respectively, with the introduction of CeB_6. These results demonstrate the advantages of inserting of CeB_6 in vertical diamond SBDs and show the potential of SBDs for future power rectifiers.

1. Introduction

Diamond is an excellent wide bandgap semiconductor for next-generation power devices due to its prominent physical and electrical properties such as high carrier mobility (electrons/ holes: 4500/3800 cm$^2 \cdot$V$^{-1} \cdot$s^{-1}), large breakdown electric field (more than 10 MV·cm^{-1}), and high thermal conductivity (2200 W·m$^{-1} \cdot$K^{-1}) [1–3]. Improvement and development of single crystal diamond growth using chemical vapor deposition techniques offer new possibilities for high-performance electronic devices, particularly diamond Schottky barrier diodes (SBDs) [4–5]. Currently, the theoretical behaviors of vertical diamond SBDs are rarely realized. However, an effective way to modify the Schottky barrier height (SBH) and improve the carriers transport across the metal–semiconductor (MS) interface is the formation of an interfacial layer [6–7]. The SBD electrical parameters, such as rectification ratio, ideality factor, reverse leakage current, and breakdown threshold, are significantly affected by inserting an interfacial layer. Nonetheless, reports on the characteristics of diamond SBDs with interfacial layers remain limited, requiring the introduction of different materials as interfacial layers to investigate diamond SBD performances.

Cerium hexaboride (CeB_6) has a high melting point (2190 ℃), good chemical stability, and low work function (2.5 eV). Thus, it has been widely used in thermionic electron sources [8]. Moreover, it exhibits more stability and has a lower work function than LaB_6 which shows an improved ability for SBDs [9]. Although CeB_6 has been studied in diamond field effect transistors [10], there have been few studies reported with CeB_6 in diamond SBDs. The excellent properties of CeB_6 make it a promising interfacial layer between MS layers, which can improve the interface state density and reduce defects for high-performance devices. In this study, an as-fabricated vertical Zr/CeB_6/p-diamond SBD with enhanced performance was obtained, demonstrating an approach to fabricating quality Schottky contacts with diamonds.

2. Device fabrication and measurement

A 3 mm × 3 mm × 0.3 mm IIb-type (1 0 0)-oriented high-pressure high-temperature P$^+$ diamond substrate with a boron concentration of 10^{20} cm^{-3} was used. Before the drift layer deposition, the diamond sample was immersed in acid and alkali solution at 250 ℃ for 1 h to remove the nondiamonds and impurities. The epitaxial layer with a

thickness of 400 nm was unintentionally grown on the diamond as the P⁻ diamond drift layer using microwave plasma chemical vapor deposition equipment [9]. The as-grown drift layer was then irradiated with UV/ Ozone for 20 min to obtain surface oxygen. Subsequently, a Ti/Pt/Au (thickness: 40/40/120 nm) multilayer was deposited on all backside of the diamond substrate using an electron beam (EB) evaporator, followed by rapid thermal annealing treatment at 450 ℃ in H_2 for 5 min to obtain an ohmic contact. Finally, a CeB_6/Zr/Au (thickness: 15/40/120 nm) diamond SBD with a round radius of 50 μm was prepared on the drift layer utilizing standard photolithography and electron beam evaporation techniques. A diamond SBD with no CeB_6 layer was fabricated on the same diamond substrate using the same experimental parameters to serve as a reference.

The characteristics of current/capacitance–voltage (J/C-V) for the diamond SBD were measured using an Agilent B1505A parameter analyzer. In addition, the presence of CeB_6 was characterized by using an X-ray photoelectron spectrometer (XPS). Fig. 1 shows side view schematics of diamond SBDs and their reference.

3. Results and discussion

XPS analysis was used to determine the composition of CeB_6. Fig. 2 (a) shows two peaks for Ce $3d_{5/2}$ and Ce $3d_{3/2}$ spectra. The binding energies for Ce $3d_{5/2}$ and Ce $3d_{3/2}$ were estimated as 885.7 and 904.4 eV, respectively. The B 1 s spectrum in Fig. 2(b) contains boride and boron-oxides, with a peak at 187.8 eV corresponding to the boron contained in CeB_6, and a peak at 191.4 eV, which might be due to the BO_x of sub boron-oxides [11]. The XPS results show evidently peaks of Ce 3d and B 1 s, demonstrating a successful CeB_6 deposition.

Fig. 3(a) exhibits the current density–voltage (J-V) characteristics of the diamond SBD on a semilog-scale. Maximum forward current densities (J) of 97.45 and 12,738 A/cm^2 for SBDs with and without CeB_6, respectively, at 10 V were obtained. Although the SBD without CeB_6 had a higher maximum forward current density, it also showed a higher reverse leakage current. The SBDs with CeB_6 showed good rectifying behavior with rectification ratios of 1.503×10^7, better than that of 1.626×10^6 at ± 10 V for SBDs without CeB_6. The insertion of CeB_6 resulted in an improved rectification ratio and decreased leakage current compared with the reference sample. The result implies that CeB_6 insertion suppresss the reverse current significantly. Based on Cheung's model [12], the ideality factor (n)/SBH (Φ_B) values were calculated as 2.24/1.92 eV and 2.82/1.65 eV for SBDs with and without CeB_6, respectively, a distinct improvement. Moreover, the turn-on voltages of the SBDs with and without CeB_6 were 2.85 and 2.15 V at 1 A/cm^2, respectively, showing an increase in the turn-on voltage with the introduction of CeB_6. From Fig. 3(b), the reverse breakdown voltages of the diamond SBDs with and without CeB_6 were measured as −110.5 and −86 V, respectively. Fig. 3(b) also indicates that the leakage current of the SBD without CeB_6 increased dramatically with an increase in the reverse voltage. Conversely, the SBD with CeB_6 exhibited a significant
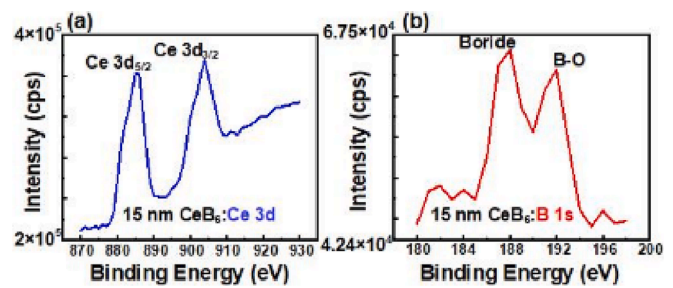

Fig. 2. XPS results of CeB_6 (a) Ce 3d, (b) B 1 s for the 15 nm thickness film.

increment in the leakage current only until the reverse voltage became greater than −64.5 V. The abnormal change in the leakage current may be ascribed to the recombination current resulting from the electron occupied interfacial states. The 28.5% enhancement of the reverse breakdown voltage and suppression of leakage for the SBD with CeB_6 suggests that introducing CeB_6 can improve the breakdown voltage by adjusting the SBH. The J-V curves in Fig. 3 indicate that the insertion of the CeB_6 layer can enhance the SBD performance. We expect further improvement with annealing treatment because the performance of an SBD with an LaB_6 interfacial layer is worse than that in an SBD with CeB_6 but becomes better than that in SBD with CeB_6 after annealing treatment [13].

Fig. 4 shows the C^{-2}-V properties of the vertical diamond SBD with CeB_6 and the reference SBD at 500 KHz. The carrier concentrations (N_A) of SBDs with and without CeB_6 were estimated as 2.646×10^{14} and 1.135×10^{14} cm^{-3}, respectively. Additionally, the widths of the depletion region were calculated as 227.6 and 206.7 nm for SBDs with and without CeB_6, respectively. The discrepancies between the carrier concentrations for SBDs with and without CeB_6 are mainly due to the existence of introduced interfacial states [9]. According to the C-V results, the values of V_{bi}/SBH were calculated as 4.064/4.322 V and 1.915/2.141 V for the SBD with and without CeB_6, respectively. The values calculated from the C-V results are higher than those from the I to V results which can be explained by the existence of excess capacitance in the devices due to CeB_6 or interface states at the Zr/CeB_6/diamond interface. And other explanation is the inhomogeneity of the Schottky interface [14].

4. Conclusions

Vertical diamond SBDs with and without CeB_6 were fabricated and characterized. The results demonstrated improved performances when introducing the CeB_6 interfacial layer. The SBDs with and without CeB_6 showed rectification ratios of 1.503×10^7 and 1.626×10^6 at ± 10 V, respectively. The device with CeB_6 demonstrated a 20.5% improvement in ideality factor and a 16.4% increase in SBH compared with the values obtained without CeB_6. In addition, the reverse breakdown voltage was enhanced from −86 to −110.5 V with the introduction of the CeB_6 layer, and the leakage current was suppressed. These results suggest that the CeB_6 layer can potentially improve the performance of high-power electronics.

CRediT authorship contribution statement

Tian-Fei Zhu: Conceptualization, Data curation, Formal analysis, Investigation, Methodology, Visualization, Writing – original draft, Visualization, Funding acquisition. **Guoqing Shao:** Investigation, Methodology, Data curation. **Tai Min:** Supervision. **Hong-Xing Wang:** Resources, Supervision, Writing – review & editing, Project administration, Funding acquisition.
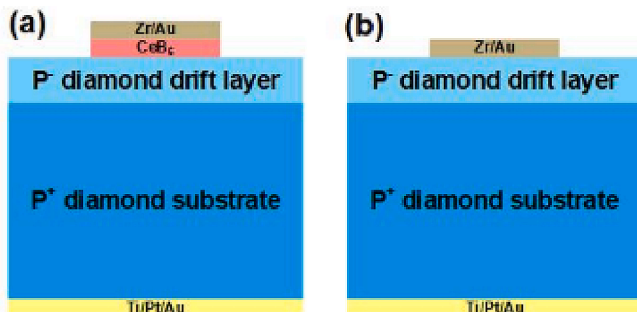

Fig. 1. Schematic diagrams of diamond SBD (a) with CeB_6 and (b) reference sample.
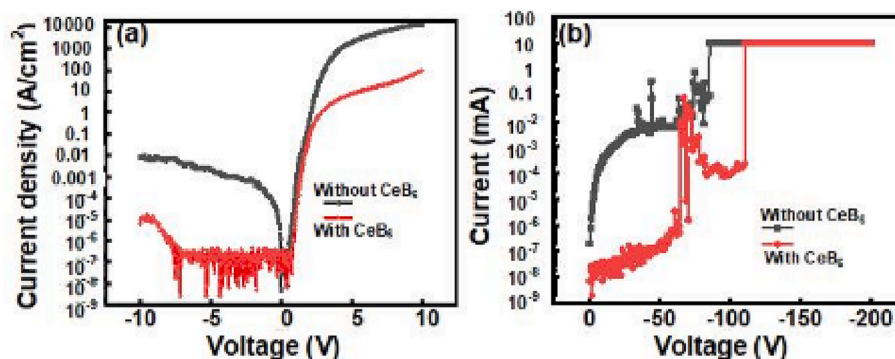
Fig. 3. (a) J-V characteristics on semilog-scale and (b) reverse semilog I-V characteristics of diamond SBD with CeB_6 and its reference, respectively.
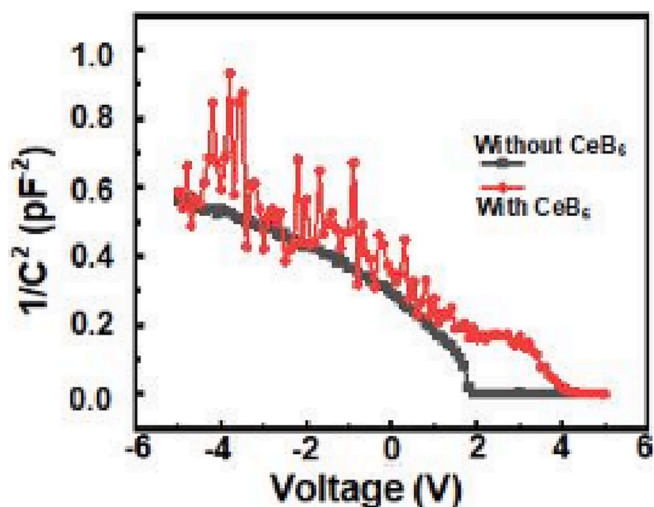

Fig. 4. C^{-2}-V characteristics of diamond SBDs with and without CeB_6 at 500 KHz.

Declaration of Competing Interest

The authors declare that they have no known competing financial interests or personal relationships that could have appeared to influence the work reported in this paper.

Data availability

Data will be made available on request.

References

[1] J. Pernot, S. Koizumi, Appl. Phys. Lett. 93 (2008), 052105, https://doi.org/10.1063/1.2969066.
[2] A.Q. Huang, IEEE Electron Device Lett. 25 (2004) 298–301, https://doi.org/10.1109/LED.2004.826533.
[3] J. Isberg, J. Hammersberg, E. Johansson, T. Wikström, D.J. Twitchen, A. J. Whitehead, S.E. Coe, G.A. Scarsbrook, Science 297 (2002) 1670–1672, https://doi.org/10.1126/science.1074374.
[4] H. Umezawa, Y. Mokuno, H. Yamada, A. Chayahara, S.-I. Shikata, Diam. Relat. Mater. 19 (2010) 208–212, https://doi.org/10.1016/j.diamond.2009.11.001.
[5] T. Funaki, K. Kodama, H. Umezawa, S. Shikata, Mater. Sci. Forum 679–680 (2011) 820–823, https://doi.org/10.4028/www.scientific.net/MSF.679-680.820.
[6] İ. Taşçıoğlu, U. Aydemir, Ş. Altındal, J. Appl. Phys. 108 (2010), 064506, https://doi.org/10.1063/1.3468376.
[7] Ş. Altındal, H. Kanbur, A. Tataroğlu, M.M. Bülbül, Phys. Rev. B Condens. Matter. 399 (2007) 146–154, https://doi.org/10.1016/j.physb.2007.06.002.
[8] T. Kusunoki, T. Hashizume, K. Kasuya, N. Arai, J. Vac. Sci. Technol. 39 (2021), 013202, https://doi.org/10.1116/6.0000739.
[9] G. Shao, J. Wang, Z. Liu, Y. Wang, W. Wang, H.X. Wang, IEEE Electron Device Lett. 42 (2021) 1366–1369, https://doi.org/10.1109/LED.2021.3099507.
[10] M. Zhang, W. Wang, G. Chen, F. Wen, F. Lin, S. He, Y. Wang, L. Zhang, S. Fan, R. Bu, T. Min, C. Yu, H. Wang, Carbon 201 (2023) 71–75, https://doi.org/10.1016/j.carbon.2022.08.056.
[11] X. Liu, T. Zhu, Y. Gong, ACS Appl. Nano Mater. 2 (2019) 5704–5712, https://doi.org/10.1021/acsanm.9b01206.
[12] S.K. Cheung, N.W. Cheung, Appl. Phys. Lett. 49 (1986) 85–87, https://doi.org/10.1063/1.97359.
[13] G. Shao, J. Wang, S. Zhang, Y. Wang, W. Wang, H.-X. Wang, Diam. Relat. Mater. 132 (2023) 109678, https://doi.org/10.1016/j.diamond.2023.109678.
[14] H.W. Jürgen, H.G. Herbert, Phys. Scri. 1991 (1991) 258, https://doi.org/10.1088/0031-8949/1991/T39/039.